

INVESTIGATION OF PHASES DEVELOPED IN $\text{Bi}_4\text{Ti}_3\text{O}_{12}$ SYSTEM BY THERMAL AND ANALYTICAL TECHNIQUES

S. NAZ, M. SHAHZAD, *A. H. QURESHI, H. WAQAS, N. HUSSAIN, K. SAEED and L. ALI¹

Materials Division, Directorate of Technology, PINSTECH, Nilore, Islamabad, Pakistan

¹Department of Metallurgical & Materials Engineering, University of Engineering and Technology,

Lahore, Pakistan

(Received May 04, 2011 and accepted in revised form May 17, 2011)

Bismuth titanate ($\text{Bi}_4\text{Ti}_3\text{O}_{12}$) powders were prepared by conventional mixed oxide method using oxide mixture i.e. bismuth oxide (Bi_2O_3) and titanium oxide (TiO_2). The mixed powders were ball milled for different times (8, 16, and 24h). The phase formation was investigated by X-ray diffraction (XRD) and results revealed that milled powder was mainly consisted of phases Bi_2O_3 , TiO_2 and small amount corresponded to $\text{Bi}_4\text{Ti}_3\text{O}_{12}$. However, after calcination at 700°C , $\text{Bi}_4\text{Ti}_3\text{O}_{12}$ phase was mainly observed. Thermal decomposition behavior (DSC-TGA-DTA) was investigated as a function of milling time. Thermal analysis alongwith XRD results showed that the formation of desire phase ($\text{Bi}_4\text{Ti}_3\text{O}_{12}$) was only possible above 600°C . Single phase $\text{Bi}_4\text{Ti}_3\text{O}_{12}$ ceramic was obtained with the orthorhombic structure by sintering at 800°C . Maximum density ($8.61\text{g}/\text{cm}^3$) was achieved in sample milled for 24h due to reduction in particle size which ultimately enhanced the diffusion process during sintering.

Keywords: Bismuth titanate, Ball milling, shrinkage behavior, XRD, DSC, DTA, TG

1. Introduction

Bismuth titanate (BIT) $\text{Bi}_4\text{Ti}_3\text{O}_{12}$ ceramics are ferroelectric materials have high breakdown strength, Curie temperature (675°C) and dielectric constant [1-3]. $\text{Bi}_4\text{Ti}_3\text{O}_{12}$ has been studied by various investigators for its ferroelectric, piezoelectric and electrooptic switching behavior. It has wide application in the electronic industry as capacitors, memory devices, sensors etc. It has a monoclinic structure at room temperature and turns into tetragonal structure above the Curie temperature (675°C). High Curie temperature enables its utilization for high temperature piezoelectric device. Moreover, it is considered to be a promising lead-free and environmentally friendly material alternative to lead zirconate titanate (PZT) [1, 4-7]. The simple and cheap technology for making such materials is well known conventional mixed oxide method, consisting of thoroughly mixing the stoichiometric oxides in ball mill, followed by calcination and finally sintered at suitable temperature. Thermal analysis techniques are very promising to obtain the evidence of intermediate phases, thermal decomposition and

sintering behavior of ceramic materials. Thermal decomposition behavior has been studied by Zaremba et al. [8,9] for the $\text{Bi}_4\text{Ti}_3\text{O}_{12}$, $\text{Na}_{0.5}\text{Bi}_{0.5}\text{TiO}_3$ and $\text{K}_{0.5}\text{Bi}_{0.5}\text{TiO}_3$. They found in DTA curves that endothermic effect of $\text{Bi}_4\text{Ti}_3\text{O}_{12}$ (BIT) in case of mechanically homogenized mixtures was at about 660°C .

Based on previous studies, it is explored that thermal analysis techniques have not been exploited in detail to investigate growth of different phases during synthesis of BIT ceramics prepared by conventional mixed oxide method. This research attempts to investigate the formation of different phases, which are ultimately responsible for the growth of $\text{Bi}_4\text{Ti}_3\text{O}_{12}$ orthorhombic phase, by thermogravimetry (TG), differential thermal analysis (DTA) and differential scanning Calorimetry (DSC) techniques. Other analytical techniques such as X-ray diffraction (XRD) and Fourier transform infrared (FTIR) spectroscopy were also employed to correlate the results with thermo analytical techniques.

* Corresponding author : ammad@pinstech.org.pk

2. Experimental

The flow chart to synthesize bismuth titanate $\text{Bi}_4\text{Ti}_3\text{O}_{12}$ powders by mixed oxide method is shown in Fig. 1. High purity Aldrich grade bismuth oxide ($\alpha\text{-Bi}_2\text{O}_3$, monoclinic structure) and titanium oxide (TiO_2 ; anatase) were weighed in stoichiometric proportion to give $\text{Bi}_4\text{Ti}_3\text{O}_{12}$. These oxides were wet ball milled for 8, 16 and 24 h and dried in an oven for 1h. The samples were designated as BT8, BT16 and BT24. The dried powders were calcined in air at 700°C for 2h. The calcined powder alongwith binder [polyethylene glycol (PEG)] was again ball milled in order to de-agglomerate and further reduced the particle size prior to compaction and sintering process. The milled powders were dried for $\frac{1}{2}$ h in an oven, pressed and sintered at 800°C for 1h each in air using covered crucible to avoid the loss of bismuth. Thermal stability of the oxide mixture and its decomposition products and phases were studied by Differential Thermal Analysis (DTA), Thermogravimetric (TG) and Differential Scanning Calorimetry (DSC) were measured with SDT Instrument Q600, USA at heating rate of $20^\circ\text{C min}^{-1}$ under a 100 mL min^{-1} flow rate of nitrogen over the temperature range of ambient to 800°C .

The calcined oxide powders of $\text{Bi}_4\text{Ti}_3\text{O}_{12}$ were used for pellet fabrication. The pellets were compacted using uniaxial hydraulic press of load capacity 10 ton/in^2 ($1 \text{ ton/in}^2 = 15.444 \text{ MPa}$). In order to obtain the single orthorhombic $\text{Bi}_4\text{Ti}_3\text{O}_{12}$ phase, the green pellets were sintered in Muffle furnace (static air) at 800°C for 1h. The sintered density of the samples was measured by Archimedes Principle. X-ray diffraction patterns at different stages were acquired from a Geigerflex D/Max-3B (M/S Rigaku Corporation, Japan) powder diffractometer with nickel filtered $\text{CuK}\alpha$ source. Powder patterns were taken in step mode at an interval of 0.05° and counting time of 2s in the range $10\text{--}80^\circ$. Fourier transform infrared (FTIR) spectra were acquired using a FTIR spectrophotometer (Nicolet 7600, Thermo- Fisher, USA) to $400\text{--}1000\text{cm}^{-1}$.

3. Results and Discussion

3.1. Powder Preparation

Thermal analysis (TG/DTA/DSC) shown in Fig. 2(a-c) was executed to determine the weight loss percent, decomposition temperature and phase

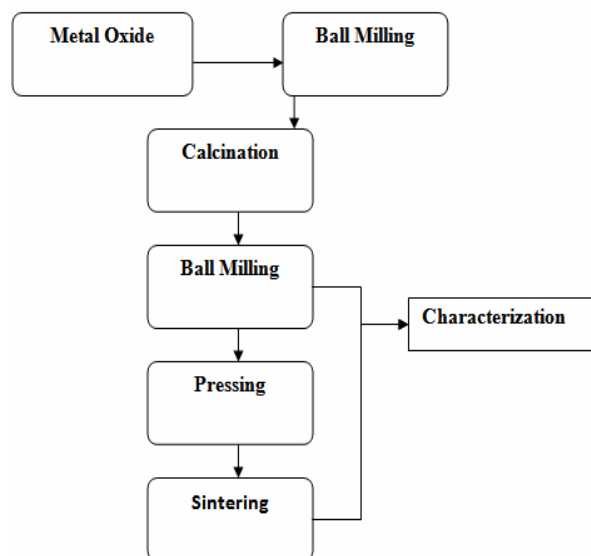


Figure 1. Flow chart to synthesize $\text{Bi}_4\text{Ti}_3\text{O}_{12}$ by conventional mixed oxide method.

transition of powder samples (BT8, BT16 and BT24) calcined at 700°C .

TG curves Fig. 2a shows total mass loss in two temperature regions of 300 to 400°C and 400 to 610°C followed by a plateau. The first mass loss corresponds to the decomposition of PEG (binder added during ball milling of calcined powder) [10, 11]. The mass loss (%) of first stage found from TG curves for BT8 and BT16 are almost same (1.6%). However, for BT24, higher mass loss (3%) was observed. This could be due to decrease in the particle size. As the particle size decreases, the surface area increases, therefore by increasing the milling time the concentration of trap binder also increases. In the second stage (400 to 610°C) minor mass loss (about 0.5%) was observed for BT8 sample, while in BT16 and BT24 samples 1% and 1.5% mass losses were observed respectively. The DTA curves (Fig. 2b) clearly indicate that there exists one endothermic reaction with onset point at 670°C . It can be observed also in the TG curve, that the process of decomposition starts at 300 and ends at 610°C and above which the mass loss becomes negligible. These results revealed that the decomposition reaction has finally ended above 600°C .

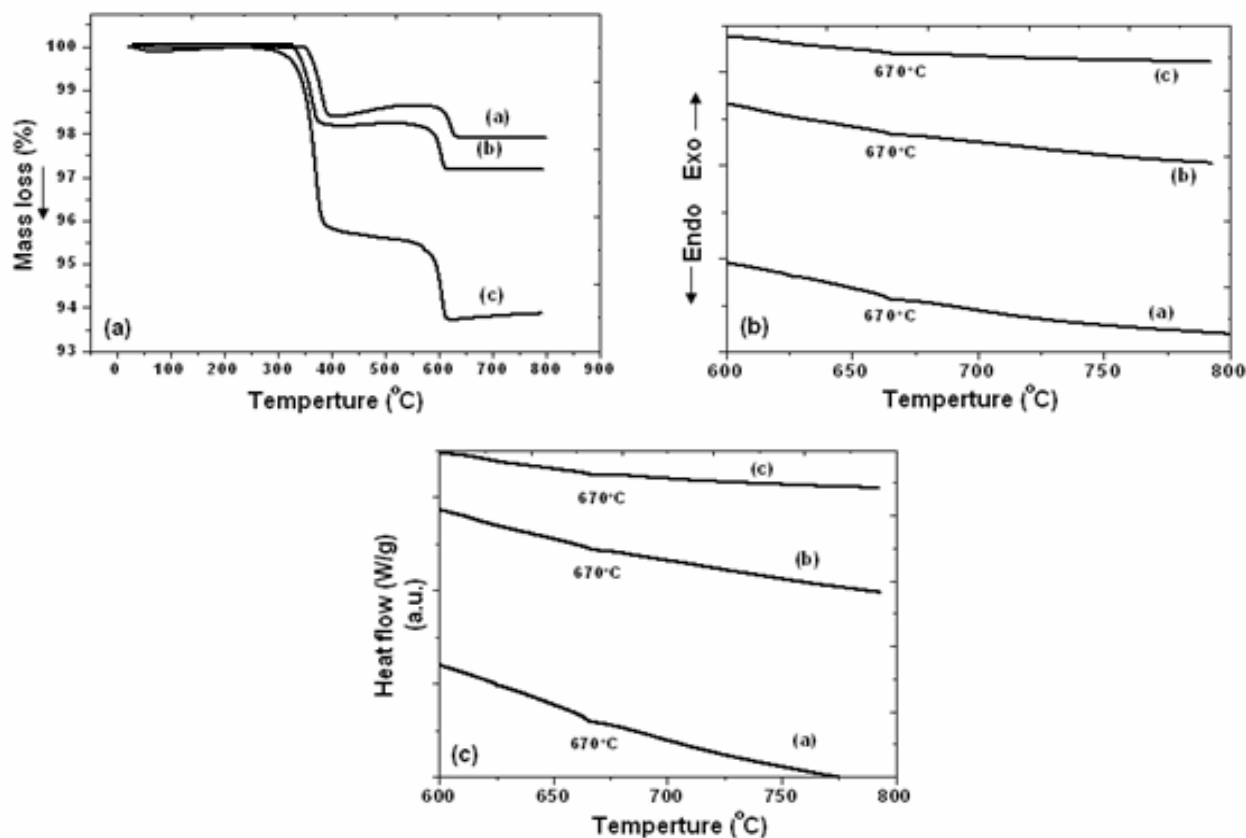


Figure 2 (a-c). Thermal analysis curves of $\text{Bi}_4\text{Ti}_3\text{O}_{12}$ powder samples BT8, BT16 & BT24 calcined at 700°C (a) TG (b) DTA and (c) DSC.

Differential Scanning Calorimetry (DSC) analysis was used to predict the polymorphs of Bi_2O_3 and Fig. 2c displays the resulting thermogram. A small endothermic peak at approximately 670°C indicates the polymorphic transformation of $\alpha \rightarrow \delta$ Bi_2O_3 and $\text{Bi}_4\text{Ti}_3\text{O}_{12}$ phase formation, which is in agreement with the data reported in literature [12,13]. As already mentioned that minor mass loss (0.5 to 1.5 percent) was observed in the second stage (400 to 610°C) of TG thermogram in Fig. 2a, which could be correlated with phase transition of Bi_2O_3 from monoclinic crystal structure (α - Bi_2O_3) to cubic fluorite type crystal structure (δ - Bi_2O_3). The α -phase exhibits p-type electronic conductivity at room temperature which transforms to n-type conductivity between 550°C and 650°C , depending on the oxygen partial pressure. The δ - Bi_2O_3 has a defective fluorite-type crystal structure in which two of the eight oxygen sites in the unit cell are vacant [12]. Theoretical mass loss of two oxygen atoms should be 1.5 percent. In present investigation almost the same

mass loss percentage was found. It has been studied [14] that Bi_2O_3 undergoes a reaction towards a cubic Bi_2O_3 by 600°C and TiO_2 decomposes by 700°C , which are ultimately responsible for the growth of $\text{Bi}_4\text{Ti}_3\text{O}_{12}$ phase. These results revealed that the formation of desire phase ($\text{Bi}_4\text{Ti}_3\text{O}_{12}$) is only possible around 700°C .

Other confirmation about the phases decomposed at different stages was obtained by XRD analysis shown in Fig. 3(a-b). The pattern, Fig. 3a, of ball milled powder sample BT16 that is without any heat treatment is mainly consisted of phases Bi_2O_3 , TiO_2 and small amount corresponds to $\text{Bi}_4\text{Ti}_3\text{O}_{12}$. After heat treatment (calcined) at 700°C , $\text{Bi}_4\text{Ti}_3\text{O}_{12}$ phase is observed in XRD patterns of samples BT8, BT16 and BT 24 shown in Fig. 3b. These results are in agreement with thermal analyses that powder is stable and desire phase ($\text{Bi}_4\text{Ti}_3\text{O}_{12}$) has fully grown around 700°C .

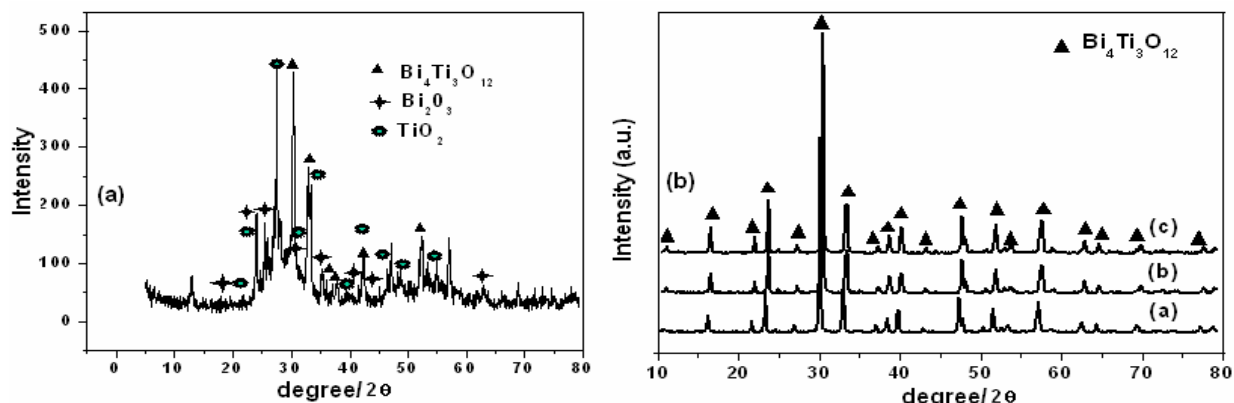


Figure 3 (a-b). XRD patterns of (a) mixed powder of BT16 sample (b) calcined powder samples (a) BT8 (b) BT16 & (c) BT24.

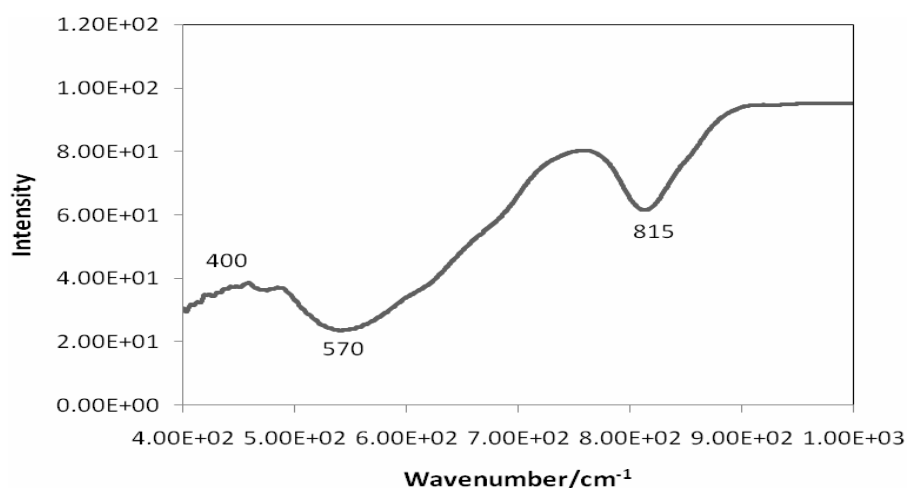


Figure 4. FTIR spectrum of calcined BT16 powder sample.

Figure 4 shows the FTIR spectrum of $\text{Bi}_4\text{Ti}_3\text{O}_{12}$ ceramic powder calcined at 700°C for sample BT16, which was recorded at room temperature. Three sharp bands were observed at 815 , 570 and 400cm^{-1} . These bands correspond to one or more characteristic bands associated to different functional groups those exist in $\text{Bi}_4\text{Ti}_3\text{O}_{12}$ [15]. The first two bands are ascribed to Ti–O and Bi–O stretching vibrations [16], while the last one belongs to Ti–O bending vibrations [17]. These results are also consistent with XRD patterns shown in Fig. 3b, supporting the fact that the formation of pure $\text{Bi}_4\text{Ti}_3\text{O}_{12}$ phase is feasible at 700°C .

3.2. Sintered Product

On the basis of thermal analysis, powder pellets were pressed and sintered at 800°C in order to obtain fully crystalline bismuth titanate phase. In pressing process binder plays a vital role to achieve the maximum value of green density. It has been observed that green density should be more than 50 percent of the theoretical density of the product. So, the selection of binder and debinding techniques is a key issue and determine the success of sintered product. In the present study polyethelene glycol (PEG) was used. It is nontoxic, widely used as water soluble binder system and has good stability along with lubricity. The binder works as glue between the particles, provides green strength and ease the process of diffusion during sintering [18].

After pressing, the green pellets were sintered at 800°C for 1h and sintered density was determined by Archimedes Principal. Figure 5 shows the variation of bulk sintered density of $\text{Bi}_4\text{Ti}_3\text{O}_{12}$ ceramic as a function of milling time. From figure it is evident that as the milling time increases bulk density increases. This increase in density is due to the decrease in particle size as a result compactness increases. From these results, it can be concluded that there is a linear relationship between milling time and density because the diffusion process during sintering enhances by close contact of particles.

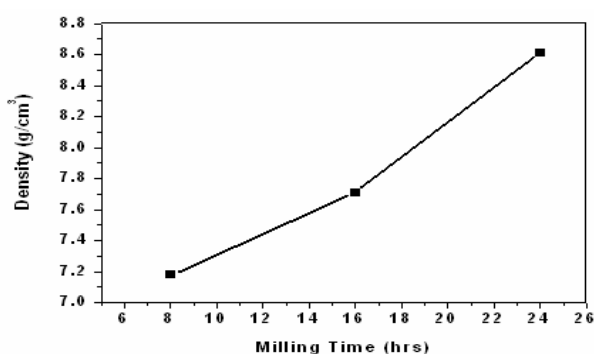


Figure 5. Variation of sintered density of $\text{Bi}_4\text{Ti}_3\text{O}_{12}$ pellets as a function of milling time.

Figure 6 (a-c) shows XRD patterns of samples BT8, BT16 and BT24 sintered at 800°C for 1h. Diffraction peaks (200)/(020), (026)/(206), (208)/(028) and (317)/(137) are separated in all three samples and split refraction of $\text{Bi}_4\text{Ti}_3\text{O}_{12}$ sintered product exhibit the change of symmetry from tetragonal to orthorhombic structure. Whereas these diffraction peaks are un-separated in calcined powders (Fig. 3b) demonstrating that $\text{Bi}_4\text{Ti}_3\text{O}_{12}$ is of tetragonal symmetry. These results are in good agreement with literature [13,19].

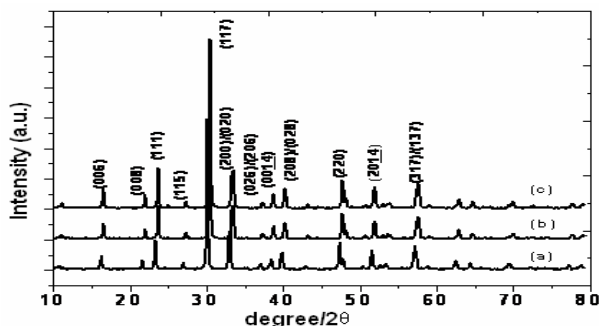


Figure 6 (a-c). XRD patterns of sintered pellets (a) BT8 (b) BT16 & (c) BT24.

These data show that milling time does produce a positive effect upon sintering. There may be an optimum time above which further milling has no significant effect on sintering.

4. Conclusions

- Bismuth titanate powders were effectively synthesized by ball milling process.
- X-ray diffraction (XRD) results revealed that milled powder contains small amount of bismuth titanate phase which completely developed after calcination.
- Thermal analysis alongwith XRD and FTIR results predicted that the formation of desire phase ($\text{Bi}_4\text{Ti}_3\text{O}_{12}$) is only possible around 700°C.
- Sintering at 800°C confirms the orthorhombic symmetry of $\text{Bi}_4\text{Ti}_3\text{O}_{12}$.
- Bulk density of sintered product increases with milling time due to decrease in particle size.

Acknowledgements

Authors gratefully acknowledge the services of Central diagnostic laboratory and XRD Lab. Of Materials Division, PINSTECH.

References

- [1] J.F. Dorrian, R.E. Newnham and K.K. Smith, *Ferroelectrics* **3** (1971) 17.
- [2] S.E. Cummings and L.E. Cross, *J. Appl. Phys.* **39** (1968) 2268.
- [3] H.S. Shulman, M. Testorf, D. Damjanovic and N. Setter, *J. Am. Ceram. Soc.* **79** (1996) 3214.
- [4] M. Billegas, C. Moure, J.F. Fernandez and P. Duran, *J. Mater. Sci.* **31** (1996), 949.
- [5] Q. Zhou and B.J. Kennedy, *Chem. Mater.* **15** (2003) 5025.
- [6] T. Takenaka and K. Sakata, *Jpn. J. Appl. Phys.* **5513** (1984) 1092.
- [7] M. Villegas, A.C. Caballero, C. Moure, P. Duran and J. F. Fernandez, *J. Am. Ceram. Soc.* **82** (1999) 2411.
- [8] T. Zaremba, *J. Therm. Anal. Calorim.* **74** (2003) 653.
- [9] T. Zaremba, *J. Therm. Anal. Calorim.* **92** (2008) 583.

- [10] J.W. Gilmanl, D.L. VanderHart and T. Kashiwagi, American Chemical Society, ACS Symposium Series 599, August 21-26, (1994), Washington, DC
- [11] L.I. Durxin, Q.U. Xuarrhui, H. Bairyun, Z. Xiaorzian, L.I. Song-Lin and L.I. Yrmim, Trans. Nonferrous Met. Soc. China **11** (2001) 90.
- [12] J.W. Medernach and R.L. Snyder, J. Am. Ceram. Soc. **61** (1978) 494.
- [13] Y. Kan, P. Wang, Y. Li, Y. Chen and D. Yan, Mater. Lett. **56** (2002) 910.
- [14] S.H. Michael, S. Speakman and S.T. Misture, JCPDS-International Centre for Diffraction Data, Advances in X-ray Analysis **45** (2002) 110.
- [15] D. Chen and X. Jiao, Mater. Res. Bull **36** (2001) 355.
- [16] H.S. Gu and A.X. Kuang, Ferroelectrics **211** (1998) 271.
- [17] N. Pavlovic, D. Kancko, K.M. Szecsenyi and V.V. Srdic, Process. Appl. Ceram. **3** (2009) 88.
- [18] M.N. Rahaman, Ceramics Processing and Sintering, Marcel Dekker, New York, (2003).
- [19] O. Yamaguchi, N. Maruyama and K. Hirota, Br. Ceram., Trans. J. **90** (1991) 111.